Inflammatory Bowel Diseases, 2026, 00(00), 1–13
https://doi.org/10.1093/ibd/izag101
Original Research Article - Translational

Preclinical development of SL-325, a novel high-affinity DR3-blocking antibody for durable inhibition of the DR3/TL1A axis in inflammatory bowel disease

Mahmud Hussain, PhD[1], Anne Y. Lai, PhD[1,‡], Derek Franklin, PhD[1,3], Karen Lenz, BS[1], Arpita Patel, BSc[1], Noah Murr, MS[1], Harunobu Kato, BA[1], Lini Pandite, MD[2,‡], Taylor H. Schreiber, MD, PhD[1,‡], Suresh de Silva, PhD[1,*,‡]

[1]Research & Development, Shattuck Labs Inc., Durham, North Carolina, United States
[2]Clinical Research, Shattuck Labs Inc., Durham, North Carolina, United States
[3]Present address: Eli Lilly and Company, California, United States

[‡]These authors contributed equally to this work.
*Corresponding author: Suresh de Silva, PhD, Shattuck Labs, Inc., 21 Alexandria Way, Suite 200, Durham, NC 27713, United States (sdesilva@shattucklabs.com).

Abstract

Background: **Death receptor 3 (DR3; also termed tumor necrosis factor receptor superfamily member 25 [TNFRSF25]) is the sole functional receptor for tumor necrosis factor (TNF)–like cytokine 1A (TL1A) and is constitutively expressed on effector lymphoid cells in peripheral blood and in both inflamed and adjacent noninflamed tissues. Excessive DR3 signaling contributes to chronic inflammation in inflammatory bowel disease (IBD). While clinical trials of anti-TL1A antibodies have demonstrated efficacy in ulcerative colitis and Crohn disease, the stable expression pattern of DR3 suggests that receptor blockade may more effectively and durably inhibit TL1A-driven proinflammatory signaling and limit disease propagation. We describe the preclinical development of SL-325, a fully human, Fc-silent, high-affinity DR3-blocking monoclonal antibody.**

Methods: **Binding affinity and specificity of SL-325 were evaluated using biophysical and cell-based assays. Functional activity was assessed in peripheral blood mononuclear cells (PBMCs) from healthy donors and IBD patients, an ex vivo human intestinal inflammation model, and cynomolgus macaque toxicology studies.**

Results: **SL-325 bound to human DR3 with picomolar affinity and high specificity while potently blocking TL1A binding without inducing DR3 agonism. SL-325 suppressed TL1A-induced proinflammatory cytokine secretion in PBMCs from healthy donors and IBD patients. In an ex vivo human intestinal model, SL-325 inhibited TL1A-driven cytokine production and preserved epithelial barrier integrity. In nonhuman primates, SL-325 was safe and well tolerated at doses up to 100 mg/kg, demonstrated dose-proportional pharmacokinetics, and led to prolonged DR3 receptor occupancy (RO) without immune activation or proliferation.**

Conclusion: **These data demonstrate that SL-325 is a novel DR3-blocking antibody with the potential to provide durable inhibition of the TL1A/DR3 axis and support the clinical development of SL-325 to treat IBD.**

Key words: DR3, TL1A blocking, SL-325, IBD, inflammation.

Introduction

There is a growing body of evidence demonstrating that genetic polymorphisms in tumor necrosis factor receptor superfamily member 15 (TNFSF15), which lead to aberrant expression of tumor necrosis factor (TNF)–like cytokine 1A (TL1A), confer susceptibility to a number of autoimmune/inflammatory and fibrotic diseases.[1,2] TL1A signals through a single receptor, most commonly referred to as DR3 (death receptor 3).[1] DR3 is constitutively expressed primarily by activated lymphocytes (T helper 1 [Th1], Th2, Th9, Th17, and regulatory T cells [Tregs])[3,4] and innate lymphoid cells (ILCs),[5,6] whereas the DR3 ligand TL1A is primarily a tissue-restricted ligand with an inducible pattern of expression on antigen-presenting cells (monocytes, dendritic cells, and macrophages) and endothelial cells in response to innate stimuli.[7,8] Under homeostatic conditions, especially in the

Received: February 23, 2026. **Accepted:** May 9, 2026

Key Messages

What is already known?

The TL1A/DR3 pathway drives intestinal inflammation in IBD, and TL1A-blocking antibodies have shown clinical efficacy in ulcerative colitis and Crohn disease.

What is new here?

To our knowledge, SL-325 is the first reported high-affinity, Fc-silenced DR3-blocking antibody demonstrating potent TL1A inhibition without agonism and with favorable safety, pharmacokinetic and receptor occupancy profiles in nonhuman primates.

How can this study help patient care?

Targeting DR3 may provide durable and differentiated inhibition of the TL1A pathway, potentially reducing immune activation risks and supporting improved therapeutic options for patients with IBD.

gut, DR3 signaling plays a dual role in both co-stimulating the foreign antigen specific effector lymphocyte response while also stimulating pre-existing Tregs to focus the clonality of immune responses and prevent bystander inflammation.[9] TL1A also directly inhibits de novo generation of Tregs, and aberrant expression of TL1A may promote autoreactivity by skewing polarization of naive T cells specific for endogenous antigens toward effector rather than regulatory lineages.[3,10,11] This biological process may contribute to the association of the TL1A/DR3 axis in a growing number of inflammatory and immune-mediated diseases, including IBD, rheumatoid arthritis, psoriasis, primary biliary cholangitis, ankylosing spondylitis, hidradenitis suppurativa, and systemic sclerosis.[2,12–17] Furthermore, DR3 expression has been observed in tissue myofibroblasts, and DR3 signaling was shown to play a direct fibrogenic role in addition to the promotion of fibrosis secondary to chronic inflammation.[2]

While it has been clear for decades that DR3 signaling potentiates inflammation in preclinical models,[18,19] the role of the axis in modulating regulatory T cells and preventing bystander inflammation has raised uncertainty for clinical studies in humans regarding when and whether inhibition of the axis would definitively suppress inflammation and provide clinical benefit. Three separate TL1A blocking antibodies have now been reported to be associated with similar placebo-adjusted remission rates in patients with ulcerative colitis (UC) and Crohn disease (CD), without evidence of significant adverse events in randomized Phase II clinical trials.[20–22] These consistent clinical results provide compelling evidence that, at least in UC and CD, TL1A signaling predominantly drives immunopathology and any reduction in TL1A signaling to Tregs does not reduce clinical benefit.

The evidence supporting DR3 signaling in the pathogenesis of intestinal inflammation in IBD includes the following: (1) significantly elevated expression of TL1A and DR3 in intestinal tissue of patients with IBD compared to healthy controls[23]; (2) correlation of the high mucosal expression of TLIA and DR3 in inflamed areas of the mucosa with the severity of inflammation, especially in patients with Crohn disease[23]; (3) association of polymorphisms in the TNFSF15 gene (which encodes TL1A) with susceptibility to Crohn disease[24,25]; (4) transgenic mice with constitutive TL1A expression in antigen presenting cells show intestinal inflammation and fibrosis whereas blockade of TL1A/DR3 suppresses chemically induced murine colitis, and (5) DR3-deficient mice are protected from intestinal inflammation even after colitis is induced.[18,19] Importantly, in a spontaneous mouse model of CD-like ileitis, referred to as the SAMP/YitFC model, whole-body genetic knockout of the DR3 receptor, which ablated TL1A signaling, resulted in the complete prevention of these mice from developing gastrointestinal inflammation and CD-like ileitis compared to TL1A knock-out SAMP/YiTFc mice, in which only the onset of the disease was delayed and the same level of protection was not conferred.[18] These experimental mouse disease model data suggest that blockade of the DR3 receptor and signaling could be more efficacious in propagating inflammatory diseases such as CD due to its constitutive expression pattern over the transient nature of its ligand, TL1A.

TL1A, the sole known signaling ligand for DR3, is initially expressed as a membrane-bound protein; however, enzymatic cleavage by the TNFα-converting enzyme (TACE; also known as ADAM17) at a membrane-proximal protease cleavage site resuls in shedding of a soluble form of TL1A (monomeric and trimeric forms) comprising the extracellular domain, which is detectable in human serum and is significantly elevated during inflammatory conditions. Humans have evolved a distinct gene encoding a nonsignaling, decoy receptor called DcR3 (TNFRSF6B), which is not present in rodents and functions to neutralize soluble TL1A, FasL, and LIGHT signaling proteins. Interestingly, the serum concentration of total TL1A increases following treatment with anti-TL1A antibodies, which is due to stabilization of serum TL1A through the formation of anti-TL1A antibody/soluble TL1A immune complexes.[26] These large immune complexes have been shown to induce high levels of antidrug antibody (ADA) responses against anti-TL1A antibodies in clinical studies.[27] Further, the ADAs resulting from these anti-TL1A antibody/soluble TL1A immune complexes have been shown to reduce clinical response in an ADA-titer–dependent manner during the induction phase of treatment.

To our knowledge, no DR3-blocking antibodies have been evaluated in clinical trials to date. Herein, we describe the preclinical characterization of a novel, fully human, and fully Fc-silenced DR3 blocking antibody, SL-325. This antibody has demonstrated epitope-specific TL1A blocking effects in primary immune cell–based assays and in an ex vivo intestinal model of inflammation without inducing agonistic effects that have translated in nonhuman primate (NHP) studies with a favorable safety, pharmacokinetic (PK), pharmacodynamic (PD), and immunogenicity profile.

Materials and methods

Construct generation

All monoclonal antibodies were expressed from mammalian expression vectors in engineered CHO-K1 cells (either transiently or stably transfected) followed by standard affinity chromatography–based purification. SL-325 produced for NHP studies was purified by 2 additional polishing steps using standard chromatography. Recombinant proteins were purchased or custom ordered from the respective vendors as indicated.

Surface Plasmon Resonance

A surface plasmon resonance (SPR) assay was performed in a Biacore 8K SPR instrument. Human DR3 (6-histidine [HIS]-tagged, Acro Biosystems) was conjugated to biotin at a 1:1 protein to biotin ratio using EZ_link NHS-Biotin (ThermoFisher) following the manufacturer's protocol. Biotin-conjugated human DR3 (50 nM) was immobilized on a streptavidin chip (Cytiva). Next, serially diluted SL-325 was flowed as the analyte at successively lower to higher concentrations for 2 minutes at each concentration. A single dissociation step was employed at the end for 10 minutes in the assay buffer (PBS-*P* + buffer, Cytiva). SPR data were analyzed by Biacore Insight Evaluation software and plotted using GraphPad Prism. Flow rate of all samples and buffers were set at 30 µL/min and the assay was run at 25 °C.

Meso Scale Discovery assays

Binding to TNFR1, TNFR2, and DcR3

Standard assay plates (L15XA-3, Meso Scale Discovery [MSD]) were coated overnight at 4 °C with 35 μL/well HIS-tagged human TNFR1, TNFR2, or DcR3 protein (2.5 µg/mL, Acro Biosystems). The next day, plates were washed 3 times with 300 µL TBST buffer and SL-325 or human TNFα-Fc (for TNFR1- or TNFR2-coated plates) or biotin-conjugated SL-325 or human TL1A (Acro Biosystems) were titrated on TNFR1- or TNFR2- or DcR3-coated assay plates followed by 3 washes with 300 µL TBST. TNFR1- or TNFR2-bound SL-325 (or TNFα-Fc) was detected using 25 μL/well sulfo-tagged Kuzko-8 anti-IgG1 antibody (0.125 µg/mL, Capri1846, Thermo) while DcR3-bound SL-325 (or TL1A) was detected using 25 μL sulfo-tagged streptavidin (0.3 µg/mL; MSD). A final wash step with 300 µL TBST was performed before the addition of 150 µL/well of MSD Gold Read A buffer and the plate was read on an MSD MESO Quick Plex SQ 120 plate reader. Raw MSD data were plotted using GraphPad Prism.

Stable cell line generation and flow cytometry to assess DR3 binding specificity and TL1A blocking

A stable CHO-K1 cell line (American Type Culture Collection; ATCC) was engineered to overexpress the human DR3 protein via stable transfection of a mammalian expression vector (pcDNA3.1) encoding the DR3 cDNA sequence (NP_683866) followed by G418 antibiotic selection. Following antibiotic selection, the stable pool of DR3-expressing Chinese Hamster Ovary K-1 (CHO-K1) cells were stained with an anti-DR3 APC conjugated antibody (BioLegend, clone 4C12) and flow-sorted to generate a stable pool of cells that expressed a high level of DR3 on the cell surface. Flow-sorted CHO-K1-DR3$^+$ cells were subsequently expanded in the presence of antibiotic selection and used for cell binding and blocking experiments with SL-325 and TL1A protein as described next. CHO-K1-DR3$^+$ cells (5×10^4) were dispensed into a V-bottom 96-well plate and simultaneous competitive binding of SL-325 or anti-TL1A antibodies (duvakitug, tulisokibart, and afimkibart biosimilars purchased from MedChemExpress) at various concentrations and a fixed concentration of 100 nM biotin-conjugated TL1A-rabbit-Fc (Sino Biologicals) was performed in serum-free Iscove's Modified Dulbecco's Medium (IMDM) prior to shaking at 600 rpm at 4°C for 1 hour. The cells were then washed twice in Fluorescence-Activated Cell Sorting (FACS) buffer (DPBS + 1% BSA + 2 mM EDTA + 0.02% sodium azide) before centrifugation at 350×g. After the supernatant was removed, cells were stained with PE-streptavidin (BioLegend catalog No. 405204) in FACS buffer at a 1:200 ratio. After the incubation, cells were washed in FACS buffer prior to centrifugation and disposal of the supernatant. The cell pellet was then resuspended in FACS buffer and run on a BD Symphony A1 flow cytometer. The geometric MFIs of the PE signal bound to the DR3$^+$ cells were normalized to the blocking percentage in the presence of SL-325 or anti-TL1A antibodies and plotted using GraphPad Prism. Native DR3 binding by SL-325 was assessed using the same flow cytometry assay format with the CHOK1-DR3$^+$ cell-line with the exception of adding TL1A. Cell-bound SL-325 was detected by APC-anti-IgG1 (Jackson Immuno Research Catalog No. 109-136-088) in FACS buffer at a 1:200 ratio. Stable cell-line generation and subsequent flow cytometry–based binding of SL-325 to other human TNF receptors was also performed as described here. OX40-expressing stable cells were generated in HeLa cells while CD40-, 4-1BB–, GITR-, and LT-βR–expressing stable cell-lines were generated in CHO-K1 cells. Fluorophore-conjugated antibodies were used to confirm TNF receptor expression (BioLegend catalog No. PE-CD40 [334308], PE-41BB [309804], PE-GITR [371203], PE-LT-βR [322008], APC-OX40 [350008]). For the transient transfection of DR3 from different species, full-length human, cynomolgus macaque (cynomolgus), canine, and rat DR3 (Sequence in Table S2) were cloned with a cleavable C-terminal GFP in the mammalian expression vector pCDNA3.1(−) followed by electroporation of the DNA in HEK293 cells using a Lonza SF Nucleofactor kit in a Lonza 4D Nucleofactor X unit. After overnight expression of DR3(GFP), SL-325 was incubated with the cells at various concentrations at 4 °C for 1 hour, followed by washing and staining with APC-conjugated anti-human Fc antibody (Jackson ImmunoResearch Laboratories Inc., catalog No. 109-136-088). Cells were analyzed in a BD Symphony A1 flow cytometer.

Direct and competitive T-cell binding by SL-325 in human and cynomolgus monkey peripheral blood mononuclear cells

SL-325 binding was assessed to detect DR3 expression on various T-cell subsets in 10 individual donor human and 10 cynomolgus peripheral blood mononuclear cell (PBMC) samples

(StemCell Technologies and Odin Bioscience) using Alexa Fluor (AF)647-conjugated SL-325 across a range of concentrations. Competitive TL1A/SL-325 binding was assessed using the same donor PBMCs with a fixed concentration of 100 nM biotin-conjugated TL1A with and without preincubation with AF647-conjugated SL-325 (5 μg/mL). In total, 2×10^5 PBMCs were used in each binding reaction. Cryopreserved PBMCs were first thawed and rested overnight at 37 °C in a CO_2 incubator in RPMI media supplemented with 10% FBS. The next day, all binding experiments were performed at 4 °C for 1 hour in 1% fetal bovine serum in RPMI media, followed by washing and then incubation with BV510 viability dye and a cocktail of fluorophore-conjugated surface marker antibodies for 30 minutes at 4 °C. After washing, cells were fixed and permeabilized using eBiosciences Fixation/Permeabilization buffer and further stained with intracellular antibodies for 40 minutes at room temperature. Cells were washed after staining, followed by data acquisition in a BD LSR Fortessa flow cytometer. Cell surface staining antibodies included PE–streptavidin (TL1A binding detection), PE-Cy7–CD8 (clone SK1), BV421–CD4 (clone OKT4), BV605–CD25 (clone BC96), and BV785–CD3 (clone SP34-2); intracellular staining was performed using Alexa Fluor 488–FoxP3 (clone PCH101).

Interferon gamma and other proinflammatory cytokine release assay from human PBMCs

Individual donor PBMCs were thawed and rested overnight in Roswell Park Memorial Institute (RPMI) complete medium at 37 °C. Following recovery, PBMCs were cultured at 7.5×10^4 cells per well and suboptimally stimulated with α-CD3/α-CD28 T Cell Activator (StemCell Technologies, 0.036 μL/well) in 96-well plates (Corning). For evaluation of SL-325 activity, cells were cultured with soluble TL1A (100 ng/mL, R&D systems catalog No. 1319-TL/CF) and various concentrations of SL-325 under both antagonist conditions (with TL1A) and agonist conditions (without TL1A). In separate experiments, membrane-bound TL1A conditions were evaluated using Human Embryonic Kidney (HEK) 293-TL1A$^+$ cells or HEK293 parental cells (control, do not express TL1A) seeded at 10 000 cells per well in a 96-well plate 1 day prior to PBMC addition. In both the soluble TL1A-induced and the membrane-bound TL1A-induced PBMC assay, the interferon gamma (IFNγ) levels in the culture supernatant collected after 72 hours was quantified using a U-PLEX Human IFNγ assay kit (MSD) according to the manufacturer's protocol. For evaluation of other inflammatory cytokines, select analytes from the U-PLEX T Cell Combo (Human) was used. All MSD Plates were read in an MSD plate reader instrument connected to the Methodical Mind software. All raw data were plotted in GraphPad Prism.

Ex vivo intestinal barrier disruption assay

RepliGut culture

Human intestinal epithelial cells derived from transverse colon tissue were cultured using the RepliGut Planar Kit (Altis Biosystems). First, a 96-well precoated transwell plate was prepared by rinsing with sterile PBS. Cryopreserved region-specific human intestinal epithelial cells were thawed at 37 °C, transferred to RepliGut Growth Medium, and centrifuged at 600×g for 1 minute. Following aspiration, cells were washed once with PBS, resuspended in Cell Dissociation Solution for 3 minutes at 37 °C, and mechanically dissociated. The cell suspension was diluted in RepliGut Growth Medium, with 100 μL added to the apical compartment. RepliGut Growth Medium alone (200 μL) was added to the basal compartment of each transwell insert. Cultures were maintained at 37 °C with medium changes every 48 hours. Upon reaching 100% confluence on day 4, the medium was changed to RepliGut Maturation Medium for differentiation of the intestinal epithelial monolayer into a functional barrier model. On day 6, preactivated healthy donor PBMCs with supernatant (see next section) were transferred to the basal compartment, and SL-325 (5 μg/mL) or media control was added to the luminal compartment in RepliGut Maturation Medium. The RepliGut culture was maintained for an additional 5 days for evaluation of barrier function. Barrier function was evaluated by daily trans-epithelial electrical resistance (TEER) measurements using the EVOM Epithelial Volt/Ohm Meter 3 and STX100 Electrode Corning 96. On day 11 (5 days posttreatment), culture supernatant was collected to measure cytokine levels. A TNFα inhibitor (adalimumab) was used in an identical experimental set up to confirm that TNFα was the main cytokine driving epithelial barrier disruption in the RepliGut system.

Prestimulation of PBMCs

PBMCs from a healthy donor were thawed and rested overnight in RPMI complete media at 37 °C. Following recovery, PBMCs were stimulated at 1.5×10^5 cells per well in 200 μL of ImmunoCult XF T Cell Expansion Medium containing α-CD3/α-CD28 T Cell Activator (0.072 μL/well), soluble TL1A (100 ng/mL), and 5 μg/mL SL-325 or media control in 96-well plates. After 24 hours of culture, PBMCs, including the entire volume of the culture supernatant, were transferred to the basal compartment (bottom chamber) of the RepliGut on day 6 of the study.

TEER and cytokine analysis

The corrected TEER values (Ω^*cm^2) were calculated by multiplying the net resistance (resistance measured minus the resistance of a blank transwell) by the surface area of the transwell (0.143 cm^2). The corrected TEER values were converted to normalized TEER, using the Normalize function in GraphPad Prism, by defining 100% as the maximum corrected TEER value for each sample during the study. The TEER values were normalized to the maximum value in each well to account for well-to-well variability. Mean ± SD of the normalized TEER values for each treatment condition were plotted for time points during the treatment phase of the study using GraphPad Prism.

TNFα levels were measured using the U-PLEX Human TNFα Assay kit (MSD) following the manufacturer's instructions. Data analysis was performed using GraphPad Prism Software Version 10.2.3. A 4-parameter logistic regression was used to generate standard curves from MSD calibrators. Sample concentrations were interpolated from the standard curves. Dose-response curves were generated by plotting cytokine concentrations vs SL-325 concentrations (nM) using GraphPad Prism.

Pharmacokinetic, receptor occupancy, ADA, and immunophenotyping assays from a cynomolgus macaque toxicology study

Pharmacokinetic assay

Serum PK samples collected at different timepoints for all dose levels, including the vehicle treated group, were assayed for SL-325 concentration using a validated bioanalytical method. Briefly, 0.5 μg/mL biotinylated human DR3 [TNF5-H52H3(Acro)/BI-999(Columbia)] was coated overnight on a streptavidin plate at 4 °C. The next day, serum PK samples were processed directly or prediluted in a pooled cynomolgus serum (BioIVT) or Diluent 57 (MSD). All PK samples, calibration standard (ranging 8160 through 15.3 ng/mL with a lower limit of quantification (LLOQ) of 45.9 ng/mL and control samples (2 sets of 3 controls at 6120, 816 and 138 ng/mL) were diluted in the assay buffer (5-fold dilution of 5% Blocker A solution, MSD) with a minimum required dilution (MRD) of 40. Overnight DR3-coated plates were washed and 50 μL/well samples were added to DR3-coated streptavidin plates in duplicates. Plates were washed after 1 hour ± 10 minutes of incubation at room temperature with shaking at 700 ± 100 rpm on a plate shaker. DR3/SL-325 complex was detected using 0.25 ug/mL (35 μL/well) sulfo-tagged Kuzko-8 (Capri1846, Thermo) followed by adding Gold read buffer A (MSD). Plates were read in MESO QuickPlex SQ 120 connected to the Methodical Mind software version 1.0.37. Raw data were analyzed in MSD Discovery Workbench Software version 4.0. A 4-parameter logistic regression–derived standard curve was generated in the MSD Discovery Workbench software. SL-325 concentrations in the PK samples were back-calculated by interpolating from the standard curve and factoring in the sample predilution as necessary.

Receptor occupancy assay and immunophenotyping

Loss of anti-DR3 (clone 4C12) binding upon SL-325 treatment was used as the readout for RO. SL-325 binds to DR3 at a distinct epitope to 4C12, however SL-325 binding to DR3 provides partial steric hindrance to 4C12 binding. Thus, when cell surface–expressed DR3 molecules are bound by SL-325, the binding of anti-DR3 (clone 4C12) is attenuated. Whole-blood samples collected at selected timepoints for all dose levels, including the vehicle-treated group, were processed to analyze DR3-receptor occupancy of SL-325. Samples were first lysed with BD Pharm Lyse to deplete red blood cells (RBCs). After RBC lysis, cells were treated with Human Fc Block to prevent non-specific staining, followed by BV510 Fixable Viability Dye to exclude dead cells. Cells were then incubated with a cocktail of fluorochrome-conjugated antibodies for 30 minutes at 4 °C (reagents and antibodies listed in Table S3). Subsequently, cells were fixed and permeabilized using eBiosciences Fixation/Permeabilization buffer and further stained with intracellular antibodies for 40 minutes at room temperature. Precision Count Beads were added prior to sample analysis for absolute cell counting. Flow cytometry data were acquired using a BD LSR Fortessa flow cytometer. Background staining levels were established using an isotype control antibody in vehicle-treated and predose samples. The analysis focused on Tregs, which express the highest levels of DR3 among T-cell subsets in naive cynomolgus macaques. The percentage of DR3-positive (4C12+) Tregs was determined for each sample. Data normalization was performed using GraphPad Prism software version 10.2.3 (built-in analysis), where for each timepoint, 100% was set as the DR3+ percentage from the vehicle group at that specific timepoint, and 0% was set as the isotype control staining level (2.9%). The percent RO was calculated by subtracting the normalized values from 100.

ADA assay, quantification of cytokines and serum TL1A

Serum ADA samples collected at different timepoints for various dose levels were assayed for antidrug (SL-325) antibodies using a validated bioanalytical method. Briefly, samples were dissociated to a final 300 mM acetic acid solution followed by mixing with biotinylated and sulfo-tagged drug. Next, samples were captured in preblocked streptavidin plates (L15SA, MSD), incubated for 2 hours ± 20 min at 700 ± 100 rpm on a plate shaker. An ADA-positive control was also included in the assay. Assay plates were next washed and read after adding MSD gold read buffer A (MSD) in an MSD instrument connected to the Methodical Mind software version 1.0.37. Raw data were analyzed in MSD Discovery Workbench Software version 4.0. ADA-positive samples were further confirmed by a repeat experiment using the same procedure described above except that a second confirmatory master mix containing unlabeled SL-325 was included.

Cytokine concentrations in serum were measured using the U-PLEX T-cell combo kit (nonhuman primate [NHP]; K15095K-2) on the MSD platform. This kit was used to assess levels of GM-CSF, IFNγ, IL-2, IL-4, IL-10, IL-13, IL-17α, MIP-3α, and TNFα. Additionally, the U-PLEX antibody set for human IL-6 (B21TX-3), which cross-reacts with cynomolgus IL-6, was incorporated into the multiplex analysis. To quantify serum TL1A, standard MSD assay plates were coated with anti-TL1A antibody (tulisokibart sequence equivalent) at 4 °C overnight, followed by washing and incubating cynomolgus serum for 1 hour at room temperature. After the serum was washed off, plate-bound TL1A was detected using biotinylated goat anti-TL1A pAb (R&D Systems catalog No. BAF744) and subsequent washing and incubation with Sulfo-tagged streptavidin. Plates were read as described above. Calibrator standard and TL1A controls (Acro catalog No. TLA-H5243) were used to qualify the assay which ranged between 65 pg/mL to 11 500 pg/mL.

See the online supplementary methods section for: (1) C1q binding assay by MSD, (2) T-cell activation and proliferation assay with plate-bound SL-325, (3) ADCC reporter assay, and (4) Bio Layer Interferometry (BLI/Octet) assays for SL-325 binding to Fc gamma receptors and cynomolgus DR3 recombinant proteins.

Statistical analysis

Graphing and statistical analysis were performed using GraphPad Prism. Unless noted otherwise, the values plotted represent the mean triplicates and error bars denote SD. Statistical significance (P value) was determined using the unpaired Student t-test. Significant P values are labeled with asterisks denoting *$P < .05$, **$P < .01$, ***$P < .001$, and ****$P < .0001$.

Results

SL-325 binds to human DR3 with high affinity and specificity

The affinity of SL-325 to recombinant human DR3 (extracellular domain) was determined by Surface Plasmon Resonance (SPR) by flowing increasing concentrations of the SL-325 antibody over a fixed concentration of immobilized recombinant DR3. The equilibrium dissociation constant, K_D of SL-325 was determined to be 1.36 pM based on the k_{on} and k_{off} values from the kinetic fitting of the data (Figure 1A). Next, the ability of SL-325 to bind cell-surface expressed native DR3 and the specificity of binding was confirmed using stable mammalian cell lines engineered to express full-length DR3 protein and a panel of TNF family receptors using flow cytometry. SL-325 showed high affinity binding to only native DR3 (EC_{50} = 8 pM), but not to CD40, LTβR, 4-1BB, GITR, or OX40 (Figure 1B). In this assay system, SL-325 was shown to bind an epitope on DR3 expressing CHO-K1 cells that did not trigger DR3 internalization at either 37 °C or 4 °C (Figure S1A). Furthermore, the specificity of SL-325 binding was confirmed in a Retrogenix off-target binding array that includes 6108 individual full-length human plasma membrane proteins, secreted and cell surface–tethered human-secreted proteins, as well as an additional 403 human heterodimers transiently expressed on HEK293 cells. In this screen SL-325 was bound with high specificity to DR3 with no off-target binding effects (Figure S2).

Binding of SL-325 to primary T-cell subsets that are known to express DR3 was also confirmed using PBMCs from 10 human donors using flow cytometry. Dose-dependent binding of SL-325 to CD4+, CD8+ or CD4+ Treg populations were observed with EC_{50} values of 0.42, 0.33, and 0.22 nM, respectively, while no binding was detected on CD3-negative non–T cells that lack DR3 expression (Figure 1C). Importantly, on average only 16% - 17% of T-cell subsets expressed DR3 across the 10 healthy donor PBMCs evaluated. Additionally, MSD-based binding assays confirmed that SL-325 did not bind to recombinant TNFR1 (Figure 1D), which shares the highest homology to DR3 among TNF receptors, nor to TNFR2 (Figure 1E) or decoy receptor 3 (DcR3; Figure 1F). TNFα and TL1A recombinant proteins were used as positive controls for binding to TNFR1/2 and DcR3, respectively, in the MSD assays. Collectively, these experiments confirm SL-325 is a high-affinity DR3-specific antibody.

SL-325 blocks TL1A binding to DR3 and downstream signaling in healthy donor and IBD patient PBMCs without triggering DR3 activation

Both the membrane-bound and soluble trimeric forms of TL1A are capable of binding and costimulating the DR3 receptor

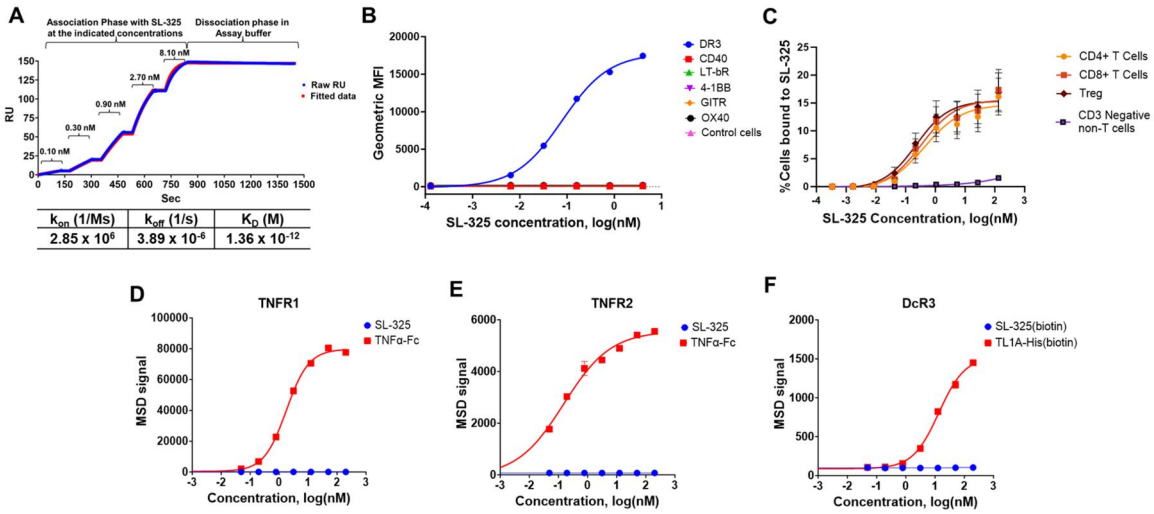

Figure 1 SL-325 binds Human DR3 with high affinity and specificity.

(A) An SPR assay with single cycle kinetics was employed to estimate the affinity of SL-325 affinity recombinant human DR3. Biotinylated human DR3 protein was immobilized on a streptavidin chip followed by flowing SL-325 at successively low to high concentrations for 2 minutes at each concentration as indicated. At the end of the association phase, a 10-minute dissociation was performed in the assay buffer. Kinetic parameters obtained from the fitted data (red trace) are shown below the kinetic profile. Data are representative of 2 independent experiments. (B) Specificity of SL-325 was assessed by testing its binding to several TNFRSF receptors by flow cytometry. $TNFR^+$ stable cells were first incubated with various concentrations of SL-325 at 4 °C followed by washing and further incubating with APC-conjugated anti-human Fc antibody to detect antibody–drug bound cells. SL-325 exhibited high affinity binding only to natively expressed DR3 with an EC_{50} of 8 pM while no detectable binding to the other TNFRSF member was observed, indicating high specificity of SL-325 toward DR3. Data points represent mean ± SD of duplicate wells. (C) Human PBMCs from 10 individual donors were incubated with increasing concentrations of fluorophore-conjugated SL-325 (0 to 132 nM) to assess direct binding to CD4+ T cells, CD8+ T cells, Tregs, and CD3 negative non-T cells by flow cytometry. Data points represent mean ± SEM of %SL-325 bound cells at each concentration. Dose-dependent binding of SL-325 to all T-cell subsets was observed. (D–F) Binding specificity of SL-325 to additional recombinantly expressed TNFRSF and decoy receptor were tested by MSD assays. The TNFRSF family proteins TNFR1 (D) and TNFR2 (E) and the decoy Receptor, DcR3 (F), were immobilized onto MSD plates and allowed to bind SL-325 (or a positive control) at various concentrations. SL-325 (to test TNFR1 or TNFR2 binding) and SL-325-biotin (to test DcR3 binding) were detected using a sulfo-tagged anti-human Fc antibody or streptavidin (or anti-HIS sulfo-tagged antibody as appropriate for the positive controls in panel F). No detectable binding to the receptors tested in the MSD assay format was observed, thus confirming the high specificity of SL-325 toward DR3. Data points represent mean ± SD of duplicate wells. APC - allophycocyanin; DcR3 - decoy receptor; DR3 - death receptor 3; Fc - fragment crystallizable; HIS - 6X histidine tag; MSD - meso scale discovery; PBMC - peripheral blood mononuclear cells; SPR - surface plasmon resonance; TNFR - tumor necrosis factor receptor; TNFRSF - tumor necrosis factor receptor super family.

expressed on T cells.[28] The ability of SL-325 to block the trimeric form of TL1A engaging with DR3 was assessed in a flow cytometry–based competitive binding assay performed with CHOK1-DR3$^+$ cells (Figure 2A). SL-325 showed complete blocking of TL1A binding to DR3 with an IC_{50} of 0.66 nM, whereas the IC_{50} of the anti-TL1A antibodies was between 5 and 20 nM. TL1A blocking potency and specificity of SL-325 were next assessed in primary immune cells. Flow-cytometry analysis of 10 human donor PBMCs demonstrated that preincubation with SL-325 provided dose-dependent inhibition of TL1A binding (Figure 2B). This differential TL1A binding across all T-cell subsets in the presence of SL-325 confirms the specificity of SL-325 to human DR3 binding as well as the TL1A blocking potency of SL-325 in PBMCs. The ability of SL-325 to block TL1A-induced downstream signaling that leads to proinflammatory cytokine release was assessed in 3 individual healthy donor PBMCs in a functional assay with primary lymphocytes expressing DR3 that were suboptimally activated with α-CD3/α-CD28 in the presence or absence of soluble TL1A (100 ng/mL) and were evaluated for cytokine production over a 72-hour assay. SL-325 completely blocked TL1A-induced IFNγ secretion in a dose-dependent manner (Figure 2C, top panel). In the absence of TL1A, the same dose titration of SL-325

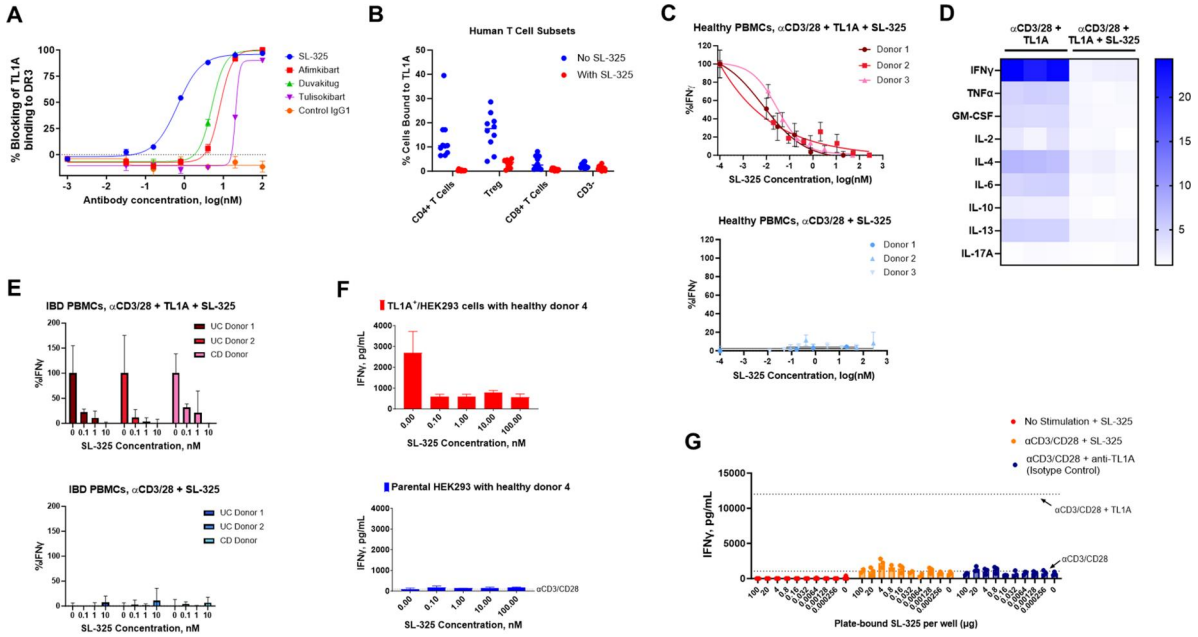

Figure 2 SL-325 blocks TL1A binding to DR3 and downstream signaling in healthy donor and IBD patient PBMCs without DR3 activation.

(A) TL1A blocking potency of SL-325 was assessed by flow cytometry. In a competitive binding assay, CHOK1-DR3$^+$ cells were simultaneously incubated with a fixed concentration (100 nM) of biotinylated human TL1A-rabbit-Fc and various concentrations of SL-325 or anti-TL1A antibodies (duvakitug, tulisokibart or afimkibart) at 4 °C for 1 hour. After washing of the cells to remove excess antibodies and TL1A, the cells were further incubated with PE-conjugated streptavidin to provide for detection of cells bound to TL1A by flow cytometry. The mean fluorescence intensity of TL1A (PE) was normalized to determine the % TL1A blocking. Data presented are mean ± SD of duplicate wells and representative of 2 independent experiments. (B) PBMCs isolated from 10 human donors were incubated with biotinylated recombinant human TL1A followed by fluorophore-conjugated streptavidin to assess cell surface DR3 expression. TL1A binding was evaluated on total CD3+ T cells, CD4+ T cells, regulatory T cells (Tregs), CD8+ T cells, and CD3− non-T cells with (red dots) and without (blue dots) preincubation with SL-325 (5 µg/mL). Binding is expressed as the percentage of TL1A-positive cells within each T-cell subset. Each dot represents an individual donor; horizontal bars indicate mean values. (C) Blocking potency of TL1A-induced IFNγ release by SL-325 was assessed in PBMC cultures. PBMCs from 3 healthy donors were stimulated with α-CD3/α-CD28 in the presence (top panel) or absence (bottom panel) of soluble trimeric TL1A (100 ng/mL). Cells were treated with increasing concentrations of SL-325 as indicated on the *x*-axis. After 72 hours, IFNγ concentrations in culture supernatants were measured by MSD immunoassay. IFNγ concentrations were normalized such that αCD3/CD28-stimulated PBMCs without SL-325 treatment were set as 0% and α-CD3/α-CD28 + TL1A-stimulated PBMCs without SL-325 treatment were set as 100%. Data shown are mean ± SD of at least 3 wells. (D) A representative heatmap showing fold change of additional cytokines in healthy donor PBMCs suboptimally stimulated with α-CD3/α-CD28 + TL1A with and without SL-325 (50 nM). Fold change of cytokines was determined by dividing the cytokine concentration in αCD3/CD28 + TL1A conditions (with or without 50 nM SL-325) by the mean concentration in α-CD3/α-CD28-stimulated conditions. Fold change of 3 replicates for each condition is shown. (E) Blocking potency of TL1A-induced IFNγ release by SL-325 was assessed in IBD patient PBMCs ($n = 3$) from 2 UC donors and 1 CD donor. PBMCs were stimulated with α-CD3/α-CD28 in the presence (top panel) or absence (bottom panel) of soluble TL1A (100 ng/mL). Cells were treated with increasing concentrations of SL-325 as indicated on the *x*-axis. After 72 hours, IFNγ concentrations in culture supernatants were measured by MSD immunoassay. IFNγ concentrations were normalized such that α-CD3/α-CD28-stimulated PBMCs without SL-325 treatment were set as 0% and α-CD3/α-CD28 + TL1A-stimulated PBMCs without SL-325 treatment were set as 100%. Data shown are mean ± SD of at least 3 wells. (F) SL-325 blocks membrane-bound TL1A-mediated IFNγ release. PBMCs from a healthy donor (donor 4) were co-cultured with either parental HEK293 cells or HEK293 cells stably expressing membrane-bound TL1A. Suboptimally α-CD3/α-CD28-stimulated PBMCs co-cultured with HEK293-TL1A$^+$ cells produced markedly elevated IFNγ levels compared to those co-cultured with parental HEK293 cells. The dotted line represents the IFNγ concentrations with α-CD3/α-CD28 stimulation only in the parental HEK293 cells. Data points represent mean ± SD of at least 3 wells and are representative of $n = 2$ healthy donor PBMCs. (G) SL-325 does not trigger DR3 activation in the absence of TL1A. Healthy donor PBMCs (donor 2) were cultured in wells coated with decreasing amounts of plate-bound SL-325 (100 - 0 μg per well) under 3 different conditions: no stimulation (red circles), α-CD3/α-CD28 stimulation (orange circles), or α-CD3/α-CD28 plus anti-TL1A (blue circles). The upper dotted line indicates IFNγ levels produced with soluble TL1A plus α-CD3/α-CD28 stimulation, while the lower dotted line shows baseline α-CD3/α-CD28 stimulation. IFNγ levels in 72-hour culture supernatants were measured by MSD immunoassay. Data points represent mean ± SD of triplicate wells.

did not increase IFNγ secretion beyond the levels produced by suboptimal α-CD3/α-CD28 activation, which confirmed the lack of any DR3 activation following SL-325 binding to the receptor (Figure 2C, bottom panel). Additionally, SL-325 potently inhibited TL1A-induced secretion of other pro-inflammatory cytokines in PBMC cultures (Figure 2D), including GM-CSF, IL-2, IL-4, IL-6, IL-10, IL-13, IL-17A, and TNFα in a similar fashion as IFNγ, indicating the broad potential of SL-325 in attenuating an inflammatory cytokine response.

Next, we assessed the TL1A blocking potency of SL-325 in IBD patient PBMCs ($n=2$ UC, $n=1$ CD; patient stratification data in Table S1) using the same IFNγ release assay as described above. Suboptimal α-CD3/α-CD28 stimulation alone produced minimal IFNγ secretion at 72 hours in these IBD donor PBMCs, while costimulation with TL1A enhanced cytokine production by 6- to 11-fold, which is comparable to what was observed in healthy donor PBMCs (Figure 2E, top panel). SL-325 effectively blocked this TL1A-mediated IFNγ production, with substantial inhibition achieved at concentrations as low as 0.1 nM and near-complete inhibition at 1-10 nM across all IBD donors tested. Importantly, there was no observable agonistic effect of increase in cytokine production by SL-325 binding to DR3 in the absence of TL1A (Figure 2E, bottom panel). To assess whether SL-325 could also inhibit membrane-bound TL1A-induced cytokine responses, PBMCs from a healthy donor were cocultured with either parental HEK293 cells or HEK293 cells stably expressing TL1A (HEK293-TL1A$^+$) on the cell surface (Figure 2F). α-CD3/α-CD28-stimulated PBMCs cocultured with HEK293-TL1A$^+$ cells produced markedly elevated IFNγ levels (approximately 3000 pg/mL) compared to those cocultured with parental HEK293 cells. SL-325 demonstrated potent, dose-dependent inhibition of this membrane TL1A-induced IFNγ production. Furthermore, to assess whether SL-325 exhibited any agonistic activity through potential DR3 receptor cross-linking, PBMCs from a healthy donor were stimulated with plate-bound SL-325 across a wide concentration range (0-100 μg) in the absence or presence of α-CD3/α-CD28 stimulation (Figure 2G). While addition of soluble trimeric TL1A significantly increased IFNγ production when combined with α-CD3/α-CD28 stimulation (upper dotted line), plate-bound SL-325 did not enhance IFNγ production above baseline levels in any of the tested conditions. A similar experiment was also designed to assess whether plate-bound SL-325 induced T-cell activation or proliferation by artificial SL-325 clustering. PBMCs were cultured for 72 hours with plate-bound SL-325 at various concentrations, and CD69 (early activation marker), Ki67 (proliferation marker), and Treg frequency (%CD25+ FoxP3+ in CD4+ T cells) were assessed. In contrast to sub-optimal α-CD3/α-CD28 stimulation (horizontal dotted lines), plate-bound SL-325 did not induce CD69 expression or Ki67 upregulation in CD4+ T cells (Figure S1B), nor did it alter the frequency or activation of Tregs in CD4+ T cells (Figure S1C). These results indicate that SL-325 lacks agonistic activity even when presented in a plate-bound/cross-linked format.

SL-325 contains mutations (IgG1 L234A/L235A/G237A by EU numbering system) to eliminate binding to Fc gamma (γ) receptors. As expected, SL-325 lacked any significant binding to FcγRI, FcγRIIA, and FcγRIIIA (V176) receptors in a BLI assay (Figure S3A-C). To confirm whether this lack of binding to FcγR by SL-325 translates to the loss of antibody-dependent cell-mediated cytotoxicity (ADCC) activity in vitro, a functional assay using the Nuclear Factor of Activated T-cells (NFAT)-reporter based FcγRIIIA(CD16)$^+$ Jurkat-Lucia cell-line system (Invivogen) was performed. In this assay, after prebinding CHOK1-DR3$^+$ cells with SL-325 and its different Fc effector-competent variants at various concentrations, FcγRIIIA (CD16)$^+$ Jurkat-Lucia cells were co-cultured for 6 hours followed by detecting the luciferase signal (Figure S3D). As expected, SL-325 binding to CHOK1-DR3$^+$ cells did not induce any luciferase activity from the reporter cells. However, the control Fc competent/IgG1 wild-type framework antibody induced significant luciferase activity at levels of 0.3 nM and above. Similarly, the control anti-DR3 IgG1 LALA only framework antibody exhibited partial activation (up to 25%) of the reporter cells compared to the control Fc competent, anti-DR3 IgG1 wild-type framework antibody. These data demonstrated that the Fc mutations in SL-325 eliminated FcγRIIIA binding and the associated ADCC activity.

In addition to the lack of Fc-effector function, these Fc mutations in SL-325 were also engineered to reduce C1q binding to avoid induction of the classical complement activation pathway in humans. As shown by an MSD assay (Figure S3E), SL-325 lacks any detectable binding to C1q even at the top concentration tested (10 μg/mL) which is similar to the FDA-approved, Fc-silenced antibody drug vedolizumab (anti-$\alpha4\beta7$ integrin antibody) for the treatment of UC. On the other hand, the canonical IgG1 wild type (WT) control of SL-325 (labeled Fc competent/IgG1 WT), and another Fc-competent antibody-drug rituximab (which contains the IgG1 WT sequence) clearly showed significant binding to C1q. Notably, neonatal Fc receptor (FcRn) binding by SL-325 was unaltered in comparison to its Fc-competent IgG1 counterpart at the early endosomal pH 6.0 despite the Fc-modulating mutations (Figure S3F). Together, these results confirm that SL-325 is a fully Fc-silenced antibody which is highly potent in blocking TL1A binding to DR3 which in turn efficiently inhibits TL1A-mediated inflammatory cytokine release in healthy donor and IBD patient PBMCs without triggering any undesired agonist activity.

SL-325 inhibits TL1A-mediated intestinal barrier disruption and production of inflammatory cytokines by PBMCs in an ex vivo IBD model

The RepliGut planar system is an ex vivo, 2-dimensional planar epithelial cell model in a transwell format, wherein epithelial barrier disruption can be assessed following co-culture with activated human lymphocytes. The RepliGut intestinal model was employed to investigate the protective effects of SL-325 on intestinal epithelial barrier function in a TL1A-mediated inflammatory environment. As shown in Figure 3A, top panel, the RepliGut system was modified by introducing prestimulated PBMCs in the basal chamber of the transwell system which is separated from the apical chamber where the intestinal epithelial monolayer was cultured and monitored for preservation or disruption of the monolayer's barrier integrity. Figure 3A (bottom panel) shows the experimental timeline for evaluating SL-325 efficacy in the RepliGut system. As shown in Figure 3B, upon addition of prestimulated PBMCs to the RepliGut culture, all experimental conditions demonstrated an initial increase in TEER

(Trans-Epithelial Electrical Resistance, a measurement of the barrier integrity of a monolayer) values during the first 2 days post-treatment, indicating the continued establishment and maturation of the epithelial monolayer on the porous membrane scaffold. The control condition (no PBMCs) maintained relatively stable TEER values throughout the experiment, establishing the baseline barrier function in the absence of immune cells. Similarly, unstimulated PBMCs and α-CD3/α-CD28 stimulated PBMCs without TL1A had minimal impact on barrier integrity, with TEER measurements largely parallel to the control condition. Notably, epithelial cells exposed to stimulated PBMCs with TL1A showed a dramatic decline in barrier function at 4 to 5 days post-treatment, with TEER values dropping by 78.2% from their peak (Figure 3B). This substantial decrease in barrier integrity is consistent with a pathogenic role of TL1A-mediated inflammation in compromising the intestinal epithelial barrier, a hallmark feature of IBD[1]. On the other hand, treatment with SL-325 provided robust protection against TL1A-induced barrier disruption. In the presence of 5 μg/mL SL-325, the epithelial monolayer maintained TEER values comparable to the control conditions, even when exposed to TL1A-stimulated PBMCs. By day 5 post-treatment, the SL-325-treated group preserved 96.7% of barrier function, compared to the untreated TL1A group, which retained only 22% of maximal barrier integrity (Figure 3B). Furthermore, when corrected TEER measurements were normalized as % of pretreatment measurements 5-days post PBMC and treatment addition (Study day 11 as in the schematics shown in Figure 3A, bottom panel), SL-325 treated wells preserved the intestinal epithelial barrier significantly higher than TL1A-treated wells that were not treated with SL-325 (Figure 3C).

Analysis of pro-inflammatory cytokines in culture supernatants from the RepliGut experiments revealed that while IFNγ remained below detection limits, TNFα levels were significantly elevated in cultures containing TL1A-stimulated PBMCs compared to control (Figure 3D).[29] To validate that TNFα is upregulated upon TL1A stimulation, we confirmed that treatment with an anti-TNFα antibody (adalimumab) retained intestinal barrier integrity in the RepliGut culture system (Figure S4). Additionally, treatment with SL-325 significantly reduced TNFα production, correlating directly with the preserved barrier function observed in TEER measurements (Figure 3D). These findings demonstrate that SL-325 effectively blocks TL1A-mediated signaling in a physiologically relevant, albeit reductionist, model of intestinal inflammation. By neutralizing the interaction between TL1A and DR3, SL-325 prevents the downstream inflammatory cascade that contributes to epithelial barrier disruption.

SL-325 demonstrates a favorable safety, PK, PD, and immunogenicity profile in NHP toxicokinetic studies

A sequence alignment of the extracellular domains of human and NHP (cynomolgus macaque) DR3 confirmed 97% sequence identity, whereas alignments of human DR3 with mouse, rat or canine showed $\leq$ 62% identity (Table S2). Accordingly, SL-325 only crossreacts with cynomolgus DR3 but not with any of the other species including mouse DR3 (Figure S5). Reactivity of SL-

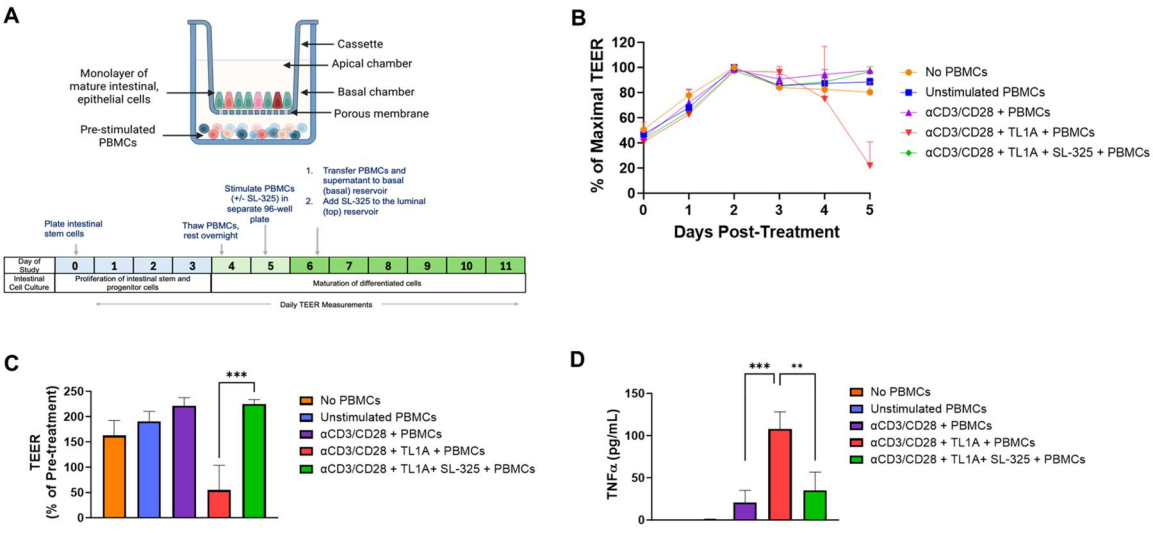

Figure 3 SL-325 inhibits TL1A-mediated intestinal barrier disruption and production of Inflammatory cytokines by PBMCs in the RepliGut ex vivo IBD model.

(A) Inhibition of TL1A-mediated intestinal barrier disruption and production of TNFα by SL-325. A sketch of the transwell culture coditions used to study the effects of SL-325 treatment on intestinal barrier function using a co-culture system of prestimulated PBMCs and the RepliGut intestinal epithelial model (top panel). The bottom panel is a schematic representation of the experimental timeline for SL-325 treatment. PBMCs derived from a healthy donor were prestimulated with α-CD3/α-CD28 complexes and recombinant TL1A to stimulate the production of inflammatory cytokines. After 24 hours, prestimulated PBMCs were added to the basal compartment of the RepliGut intestinal culture system while SL-325 (5 μg/mL) was applied to the apical compartments. (B) Intestinal barrier integrity was assessed by daily TEER measurements. Data points represent mean ± SD of the normalized TEER values for $n = 4$ biological replicates of each treatment condition. (C) TEER values on day 5 posttreatment were plotted as percentage of pretreatment values. ***P < .001 between TL1A-stimulated wells treated with and without SL-325 (D) Culture supernatants from the transwell co-culture were collected 5 days posttreatment to quantify TNFα levels. Bar graph represents mean ± SD of TNFα concentration (pg/mL) across various PBMC conditions. Statistical significance is indicated between groups: ***$P < .001$ comparing TL1A-stimulated PBMCs to unstimulated controls; **$P < .01$ comparing TL1A-stimulated PBMCs with and without SL-325 treatment.

325 to DR3 expressed on cynomolgus PBMCs was confirmed by the loss of recombinant TL1A protein binding in T cells across 10 cynomolgus donor PBMCs (Figure 4A). Therefore, cynomolgus monkey was selected as the pharmacologically relevant species to conduct toxicokinetic studies for SL-325. The toxicokinetic study was conducted over an 8-week period to evaluate safety, pharmacokinetic (PK), pharmacodynamic (PD, ie, DR3 RO) and immunogenicity profiles of SL-325. Study animals were administered either vehicle control or SL-325 by intravenous injections at 3 dose levels (1, 10 and 100 mg/kg) at the beginning of the study (day 1) with 2 subsequent repeat doses on days 15 and 29, followed by a 4-week recovery period at the highest dose (Figure 4B). Clinical pathology, hematology and histopathology analysis showed that SL-325 exposure over the 8-week study period resulted in no observable clinical or toxicologic effect on the test animals (data not shown). In addition, no SL-325 related changes in gross pathology or histopathology following necropsy were observed. As a result, the no observed adverse effect level (NOAEL) was determined to be the highest administered dose, 100 mg/kg. A dose-proportional PK profile was observed following the first dose of SL-325 (Figure 4C). SL-325 was able to fully saturate DR3 on Tregs and CD4+T cells within 24 hours across all dose levels. Full RO was maintained throughout the dosing intervals for the 10 and 100 mg/kg groups (Figure 4D, top panel). Two animals in the low dose (1.0 mg/kg) group had a decrease in RO at various timepoints (day 22 and 43) that correlated with a concomitant decrease in serum exposure due to the generation of an antidrug antibody (ADA) response (Figure 4D, bottom panel). Treatment emergent ADA were confirmed in 3/22 (13%) of SL-325 treated animals. DR3 RO was observed to decline in the 2 of 3 ADA positive animals, concurrent with a drop in SL-325 serum concentrations to between 1-177 ng/ml. Complete DR3 RO was maintained in all other animals, with the lowest observed serum concentration of 1.5 μg/mL. These results indicate that serum concentration of approximately 1 μg/ml of SL-325 were associated with full RO on DR3 in the peripheral blood compartment (Figure 4D, bottom panel).

Additionally, SL-325 and vehicle-treated animal serum were analyzed for changes in a panel of 10 pro-inflammatory cytokines at predose and post-dose 24 hours and 144 hour timepoints. The cytokines included in this analysis were: GM-CSF, IFNγ, IL-2, IL-4, IL-6, IL-10, IL-13, IL-17A, MIP-3α, and TNFα. As these were healthy animals, no elevations in any cytokines were noted in the pretreatment samples, and no changes in any of the cytokine levels were detected following SL-325 treatment, suggesting no immune activation in response to SL-325 administration (Figure S6). Similarly, no changes in circulating soluble cynomolgus TL1A levels were observed in the SL-325 dosed animals pre- and post-dose at the time points (Figure S6, bottom right panel). Furthermore, T-cell subset immunophenotyping analysis was performed on the study animals to evaluate potential effects of SL-325 treatment on T-cell activation and proliferation which was monitored through assessment of CD25 and Ki67 marker expression, respectively. Compared to vehicle control, the percentage of CD25+ or Ki67+ cells remained unchanged following SL-325 administration across all dose groups within the CD4+ T cells (Figure 4E). Notably, despite full RO of SL-325 on Tregs, there were no observable changes in either the proportion of Tregs within the CD4+ T-cell population or the percentage of Ki67+ Tregs (Figure 4F). Despite demonstrated target engagement as evidenced by the RO data, SL-325 treatment did not produce changes in T-cell activation or proliferation distinct from vehicle control at any tested dose, further confirming the lack of DR3 agonism following SL-325 binding. Overall, the NHP PK, RO, cytokine, and phenotypic data together with the observation that no test subjects had any adverse events even at the highest dose level suggests that SL-325 is safe in cynomolgus monkeys and can maintain durable DR3-engagement without triggering T-cell activation or proliferation.

Discussion

There have now been a number of instances for which the biological properties of ligand-blocking antibodies can be compared to receptor-blocking antibodies. Understandably, each instance is unique and influenced both by the inherent biology of the ligand/receptor axis being targeted and the pharmacologic properties of the antibodies being tested. Blocking antibodies directed to TNF ligands must simply provide steric hindrance to prevent receptor binding. Because TNF receptors undergo ligand-induced trimerization for activation, blocking antibodies directed to TNF receptors carry potential “agonist” liability resulting from the potential cross-linking of multiple receptor subunits from each Fab arm of a monoclonal antibody. Engineering techniques that reduce the risk of TNF receptor agonism include (1) careful selection of binding epitopes that do not cause receptor internalization, (2) recognizing the inverse relationship between agonist potential and binding affinity, and (3) removing any Fc gamma receptor binding potential. Each of these techniques was applied in the development of SL-325, described herein as a potent DR3-blocking antibody.

The binding of TL1A to DR3 causes receptor-mediated endocytosis.[29] Testing for internalization of DR3 following antibody binding likely enriched the pool of DR3 binders for clones that were less likely to demonstrate DR3 agonist effects in subsequent cell-based functional assays. In addition, stable binding to DR3 offers potential for extended dosing intervals if receptor occupancy is demonstrated to be long lasting, which appears to be the case based on data collected in the NHP toxicology studies. In IBD patients, DR3 is known to be more abundant than TL1A under inflamed conditions in peripheral blood immune cells and in the lamina propria (CD4, CD8, NK, NKT, ILC, and macrophages),[30,31] and this will lead to a higher degree of target-mediated drug disposition for the first dose of a DR3-blocking antibody relative to a TL1A-blocking antibody. However, if receptor occupancy is durable, clearance would be expected to decrease rapidly for DR3-blocking antibodies following repeat dosing. Because TL1A is a short-lived target expressed in a pulsatile manner, clearance would be expected to remain fairly constant for TL1A-directed antibodies. Given that TL1A/DR3 signaling is important in maintaining gut homeostasis and tolerance by regulating costimulatory signaling on activated T cells including Tregs, it would be important to assess the functional consequence of consistent durable DR3 blockade by SL-325 in long-term NHP studies and human studies. These properties are being evaluated in an ongoing 6-month chronic toxicology study in NHPs and in a Phase I clinical trial in healthy volunteers [NCT07158437].

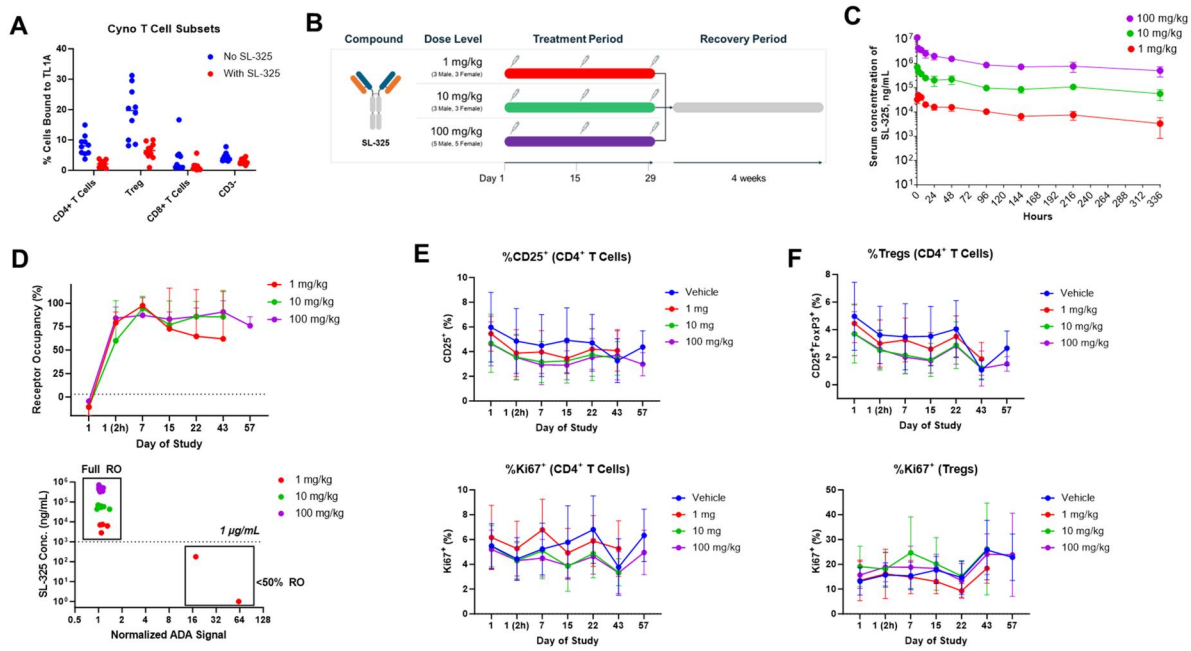

Figure 4 SL-325 is safe and well tolerated in cynomolgus macaques with no evidence of DR3 activation following receptor binding.

(A) PBMCs isolated from 10 cynomolgus macaque donors were incubated with biotinylated recombinant human TL1A followed by fluorophore-conjugated streptavidin to assess cell surface DR3 expression. TL1A binding was evaluated on total CD3+ T cells, CD4+ T cells, regulatory T cells (Tregs), CD8+ T cells, and CD3– non–T cells with (red dots) and without (blue dots) preincubation with SL-325 (5 µg/mL). Binding is expressed as the percentage of TL1A-positive cells within each T-cell subset. Each dot represents an individual donor; horizontal bars indicate mean values. TL1A binding was highest in Tregs and was significantly reduced in all T-cell subsets following SL-325 preincubation, demonstrating the specificity of TL1A binding to DR3 and TL1A blocking activity of SL-325 on cynomolgus DR3. (B) Schematic representation of a repeat dose Good Laboratory Practice (GLP) toxicology study design in cynomolgus macaques. The study was designed to administer SL-325 as an intravenous bolus injection over a 30-minute period at the beginning of the study and 2 subsequent repeat dosings at 2-week intervals at 3 dose levels including a vehicle group: 1 mg/kg, 10 mg/kg, and 100 mg/kg. Cynomolgus monkeys were grouped as 3 males and 3 females at each of the 1 mg/kg and 10 mg/kg dose levels, whereas 5 male and 5 female monkeys were dosed at the 100 mg/kg dose level (in total 32 animals including the vehicle group). A 4-week recovery period followed with a terminal necropsy analysis for the 100 mg/kg dose level. (C) Pharmacokinetic (PK) profile of SL-325 in cynomolgus macaque serum. Serum collected from all study animals at preselected time-points after SL-325 administration was analyzed by an MSD immunoassay. Biotinylated human DR3 was coated on streptavidin plates, followed by addition of prediluted serum samples in duplicate wells. DR3-bound SL-325 was detected by an anti-human Fc detector antibody. Data points represent mean ± SD of $n = 6$, $n = 6$, and $n = 10$ animals at each timepoint at 1, 10, and 100 mg/kg dose levels, respectively. (D) DR3 receptor occupancy (RO) of SL-325 in the peripheral blood of study animals (top panel). RO was determined indirectly by measuring the loss of binding of anti-DR3 antibody (clone 4C12) to Treg cells of study animals that were dosed with SL-325, which arises from the steric hindrance of 4C12 binding in the presence of SL-325. RO data was normalized to percentage binding using isotype control staining of the vehicle-group animals at each time point (detailed description in the Materials and Methods section). Analysis of SL-325 serum concentration versus normalized ADA signal in all study animals alongwith annotation of RO status (bottom panel). (E-F) Immunophenotyping of study animals to evaluate potential effects of SL-325 treatment on T-cell activation and proliferation through assessment of CD25 and Ki67 expression, respectively. Compared to vehicle control, the percentage of CD25+ cells (E, top panel) or Ki67 + cells (E, bottom panel) within the CD4 + T cells was not significantly altered by SL-325 treatment. Notably, despite high receptor occupancy of SL-325 on Tregs, there were no observable changes in either the proportion of Tregs within the CD4+ T-cell population (F, top panel) or the percentage of proliferating Ki67+ Tregs (F, bottom panel). These data indicate that throughout the course of the study, there was no activation or proliferation of CD4 + or Tregs within the CD4 + T cells.

DR3 signaling in T cells is dependent upon concurrent activation of the T-cell receptor.[32] Thus, the most sensitive methods to evaluate DR3 activation are cell-based in vitro assays or in vivo systems wherein T-cell proliferation can be observed in the presence of α-CD3/α-CD28 TCR activators or specific antigens, respectively. When evaluating potential agonist effects in the context of in vitro cell-based assays, suboptimal concentrations of α-CD3/CD28 coated beads were used to preserve the dynamic range of the assay in the presence of TL1A. When maximal concentrations of α-CD3/α-CD28 coated beads are used, proliferation and cytokine production become maximal and the costimulatory effect of TL1A becomes undetectable (data not shown). When DR3 is activated in vivo in healthy animals using TL1A protein or a agonist antibody (clone 4C12), the primary pharmacodynamic effect is proliferation of CD4+ FoxP3+ regulatory T cells.[32] This is because among all T cells, Tregs are the subpopulation that most frequently encounter cognate antigen in the form of self-antigens. The data presented herein illustrate that SL-325 lacks any evidence of DR3 agonism either in vitro in highly sensitive cell-based assays or in vivo in NHPs. Studies have shown that mononuclear cells from the lamina propria (LPMN) from IBD patients express DR3 and respond to TL1A similarly to peripheral blood immune cells.[31] Although the data provided using the RepliGut system concurs with emerging clinical data showing that TL1A is an important driver of intestinal inflammation, future studies should aim to further define the specific cell types and spatiotemporal architecture of both TL1A expression and DR3 activation using human intestinal biopsies or human organoid models. Intestinal biopsy studies from IBD patients before and after treatment with a TL1A- or DR3-blocking antibody would be particularly useful to further understand the cellular context of inflammation, and whether

there is evidence of both effector and Tregs directed to common antigens, or whether aberrant expression of TL1A may have shunted maturation of naive T cells away from Tregs in a manner that may be difficult to reverse in the absence of persistent TL1A/DR3 inhibition.

TL1A-blocking antibodies are reported to cause ADA formation in $>65\%$ of humans, which is largely driven by immune complex formation between the shed TL1A and the anti-TL1A antibodies. In NHPs, this process was reported to cause infusion-related reactions and death in the case of tulisokibart.[33] In light of these findings, it is notable that the rate of ADA formation for SL-325 in NHPs was 13%. Accordingly, there were no SL-325–related adverse events reported of any kind, no infusion-related reactions, no changes in serum or clinical chemistry analytes, and no changes in gross or histopathology findings despite achievement of complete DR3 receptor occupancy in all animals throughout the study. While SL-325 achieved full DR3 occupancy even at the lowest dose level in healthy NHP, it is anticipated that the threshold for achieving complete DR3 occupancy may be increased in humans with IBD as a result of both greater abundance of DR3-expressing lymphoid cells and increased clearance of therapeutic antibody resulting from active inflammation at the time of treatment. In aggregate, the results reported in this study suggest that given the favorable safety and pharmacologic properties of SL-325 in NHPs, SL-325 is worthy of further investigation to durably prevent TL1A-driven inflammation to treat IBD patients.

Acknowledgments

The authors would like to thank (1) the Technical Operations team at Shattuck Labs Inc., for producing the toxicology study batch of SL-325 (2) the NHP test facilities at Charles River Laboratories, United States, for conducting the NHP toxicology study (3) the Macromolecular Interactions Facilities at the University of North Carolina (Chapel Hill, United States) for facilitating SPR experiments and (4) Altis Biosystems (North Carolina, United States) for technical expertise with the RepliGut ex vivo intestinal model system.

Supplementary material

Supplementary data are available at *Inflammatory Bowel Diseases* online.

Funding

This work was supported by Shattuck Labs, Inc.

Conflicts of interest

All authors are current or former employees of Shattuck Labs, Inc. and hold an equity interest in the company.

Compliance statement

All studies were performed as per COPE and ICMJE guidelines. Compliance of all internal and externally executed studies (eg, non-human primate studies) were ensured as per regulatory agency guidelines with rigorous validation and monitoring by independent auditors as appropriate.

Article main point

SL-325 is a first-in-class DR3-blocking antibody that potently inhibits TL1A-mediated inflammatory signaling without receptor agonism. It suppresses pro-inflammatory cytokines in vitro, preserves intestinal barrier integrity ex vivo, and demonstrates favorable safety and pharmacokinetics in NHPs, supporting clinical development in IBD.

Data availability

The data underlying this article are available in the article and in its online supplementary material.

References

1. Valatas V, Kolios G, Bamias G. TL1A (TNFSF15) and DR3 (TNFRSF25): A Co-stimulatory system of cytokines with diverse functions in gut mucosal immunity. *Front Immunol*. 2019;10:583. https://doi.org/10.3389/fimmu.2019.00583
2. Bamias G, Menghini P, Pizarro TT, Cominelli F. Targeting TL1A and DR3: the new frontier of anti-cytokine therapy in IBD. *Gut*. 2025;74:652-668. https://doi.org/10.1136/gutjnl-2024-332504
3. Pappu BP, Borodovsky A, Zheng TS, et al. TL1A-DR3 interaction regulates Th17 cell function and Th17-mediated autoimmune disease. *J Exp Med*. 2008;205:1049-1062. https://doi.org/10.1084/jem.20071364
4. Richard AC, Tan C, Hawley ET, et al. The TNF-family ligand TL1A and its receptor DR3 promote T cell-mediated allergic immunopathology by enhancing differentiation and pathogenicity of IL-9-producing T cells. *J Immunol*. 2015;194:3567-3582. https://doi.org/10.4049/jimmunol.1401220
5. Longman RS, Diehl GE, Victorio DA, et al. CX(3)CR1(+) mononuclear phagocytes support colitis-associated innate lymphoid cell production of IL-22. *J Exp Med*. 2014;211:1571-1583. https://doi.org/10.1084/jem.20140678
6. Ahn YO, Weeres MA, Neulen ML, et al. Human group3 innate lymphoid cells express DR3 and respond to TL1A with enhanced IL-22 production and IL-2-dependent proliferation. *Eur J Immunol*. 2015;45:2335-2342. https://doi.org/10.1002/eji.201445213
7. Prehn JL, Thomas LS, Landers CJ, Yu QT, Michelsen KS, Targan SR. The T cell costimulator TL1A is induced by FcgammaR signaling in human monocytes and dendritic cells. *J Immunol*. 2007;178:4033-4038. https://doi.org/10.4049/jimmunol.178.7.4033
8. Migone TS, Zhang J, Luo X, et al. TL1A is a TNF-like ligand for DR3 and TR6/DcR3 and functions as a T cell costimulator.

Immunity. 2002;16:479-492. https://doi.org/10.1016/s1074-7613(02)00283-2
9. Schreiber TH, Podack ER. Immunobiology of TNFSF15 and TNFRSF25. *Immunol Res*. 2013;57:3-11. https://doi.org/10.1007/s12026-013-8465-0
10. Taraban VY, Slebioda TJ, Willoughby JE, et al. Sustained TL1A expression modulates effector and regulatory T-cell responses and drives intestinal goblet cell hyperplasia. *Mucosal Immunol*. 2011;4:186-196. https://doi.org/10.1038/mi.2010.70
11. Khan SQ, Tsai MS, Schreiber TH, Wolf D, Deyev VV, Podack ER. Cloning, expression, and functional characterization of TL1A-Ig. *J Immunol*. 2013;190:1540-1550. https://doi.org/10.4049/jimmunol.1201908
12. Song YJ, Choi IA, Meylan F, et al. Circulating TNF-like protein 1A (TL1A) is elevated early in rheumatoid arthritis and depends on TNF. *Arthritis Res Ther*. 2020;22:106. https://doi.org/10.1186/s13075-020-02198-9
13. Képíró L, Széll M, Kovács L, Keszthelyi P, Kemény L, Gyulai R. Genetic risk and protective factors of TNFSF15 gene variants detected using single nucleotide polymorphisms in Hungarians with psoriasis and psoriatic arthritis. *Hum Immunol*. 2014;75:159-162. https://doi.org/10.1016/j.humimm.2013.11.006
14. Sun Y, Irwanto A, Toyo-Oka L, et al. Fine-mapping analysis revealed complex pleiotropic effect and tissue-specific regulatory mechanism of TNFSF15 in primary biliary cholangitis, Crohn's disease and leprosy. *Sci Rep*. 2016;6:31429. https://doi.org/10.1038/srep31429
15. Konsta M, Bamias G, Tektonidou MG, Christopoulos P, Iliopoulos A, Sfikakis PP. Increased levels of soluble TNF-like cytokine 1A in ankylosing spondylitis. *Rheumatology (Oxford)*. 2013;52:448-451. https://doi.org/10.1093/rheumatology/kes316
16. Llewellyn H, Thoi L, Bogle R, Xing X, Munoz-Elias EJ, Gudjonsson J. The TL1A-DR3 axis coordinates antigen presenting cell and IL17+ T cell crosstalk in HS. Paper presented at: Inflammatory Skin Disease Summit 2025.
17. Xu W, Su L, Qing P, et al. Elevated levels of TL1A are associated with disease activity in patients with systemic sclerosis. *Clin Rheumatol*. 2017;36:1317-1324. https://doi.org/10.1007/s10067-017-3612-y
18. Butto LF, Jia LG, Arseneau KO, et al. Death-Domain-Receptor 3 deletion normalizes inflammatory gene expression and prevents ileitis in experimental Crohn's disease. *Inflamm Bowel Dis*. 2019;25:14-26. https://doi.org/10.1093/ibd/izy305
19. Li Z, Butto LF, Buela KA, et al. Death Receptor 3 signaling controls the balance between regulatory and effector lymphocytes in SAMP1/YitFc mice with Crohn's disease-like Ileitis. *Front Immunol*. 2018;9:362. https://doi.org/10.3389/fimmu.2018.00362
20. Danese S, Allegretti JR, Schreiber S, et al. Anti-TL1A antibody, afimkibart, in moderately-to-severely active ulcerative colitis (TUSCANY-2): a multicentre, double-blind, treat-through, multi-dose, randomised, placebo-controlled, phase 2b trial. *Lancet Gastroenterol Hepatol*. 2025;10:882-895. https://doi.org/10.1016/S2468-1253(25)00129-3
21. Sands BE, Feagan BG, Peyrin-Biroulet L, et al.; ARTEMIS-UC Study Group. Phase 2 trial of Anti-TL1A monoclonal antibody tulisokibart for Ulcerative Colitis. *N Engl J Med*. 2024;391:1119-1129. https://doi.org/10.1056/NEJMoa2314076
22. Jairath V, Kierkus J, Duvall GA, et al. OP40 Duvakitug (TEV-48574), an anti-TL1a monoclonal antibody, demonstrates efficacy and favourable safety as an induction treatment in adults with moderately to severely active Crohn's disease: results from a phase 2b, randomised, double-blind, placebo-controlled dose-ranging, basket trial (RELIEVE UCCD). *J Crohn Colitis*. 2025;19:i77-i78. https://doi.org/10.1093/ecco-jcc/jjae190.0039A
23. Bamias G, Martin C, 3rd, Marini M, et al. Expression, localization, and functional activity of TL1A, a novel Th1-polarizing cytokine in inflammatory bowel disease. *J Immunol*. 2003;171:4868-4874. https://doi.org/10.4049/jimmunol.171.9.4868
24. Yamazaki K, McGovern D, Ragoussis J, et al. Single nucleotide polymorphisms in TNFSF15 confer susceptibility to Crohn's disease. *Hum Mol Genet*. 2005;14:3499-3506. https://doi.org/10.1093/hmg/ddi379
25. Michelsen KS, Thomas LS, Taylor KD, et al. IBD-associated TL1A gene (TNFSF15) haplotypes determine increased expression of TL1A protein. *PLoS One*. 2009;4:e4719. https://doi.org/10.1371/journal.pone.0004719
26. Hassan-Zahraee M, Ye Z, Xi L, et al. Antitumor necrosis factor-like Ligand 1A therapy targets tissue inflammation and fibrosis pathways and reduces gut pathobionts in ulcerative colitis. *Inflamm Bowel Dis*. 2022;28:434-446. https://doi.org/10.1093/ibd/izab193
27. Kroenke MA, Barger TE, Hu J, et al. Immune complex formation is associated with loss of tolerance and an antibody response to both drug and target. *Front Immunol*. 2021;12:782788. https://doi.org/10.3389/fimmu.2021.782788
28. Zwolak A, Chan RS, Harvilla P, et al. A stable, engineered TL1A ligand co-stimulates T cells via specific binding to DR3. *Sci Rep*. 2022;12:20538. https://doi.org/10.1038/s41598-022-24984-y
29. Bittner S, Knoll G, Fullsack S, Kurz M, Wajant H, Ehrenschwender M. Soluble TL1A is sufficient for activation of death receptor 3. *Febs J*. 2016;283:323-336. https://doi.org/10.1111/febs.13576
30. Hedl M, Abraham C. A TNFSF15 disease-risk polymorphism increases pattern-recognition receptor-induced signaling through caspase-8-induced IL-1. *Proc Natl Acad Sci U S A*. 2014;111:13451-13456. https://doi.org/10.1073/pnas.1404178111
31. Llewellyn H, Aslam S, Chou T, et al. TL1A Drives TH1, TH2 and TH17 pathways in human lamina propria cells in IBD. *Gastroenterology*. 2026;170:S-1257. https://doi.org/10.1016/S0016-5085(26)03148-3
32. Schreiber TH, Wolf D, Tsai MS, et al. Therapeutic Treg expansion in mice by TNFRSF25 prevents allergic lung inflammation. *J Clin Invest*. 2010;120:3629-3640. https://doi.org/10.1172/JCI42933
33. SEC. Form S-1 Registration Statement by Prometheus Biosciences, Inc. In: U.S. Securities and Exchange Commission; 2021.

Inflammatory Bowel Diseases, 2026, 00, 1–13
https://doi.org/10.1093/ibd/izag101
Original Research Article - Translational